

Percolation effects in immiscible displacement

David Wilkinson

Schlumberger-Doll Research, Old Quarry Road, Ridgefield, Connecticut 06977-4108

(Received 14 February 1986)

The observable consequences of percolation models of immiscible displacement in porous media are discussed, with emphasis on the critical behavior. At the microscopic level, these include the fractal nature of the nonwetting fluid configuration at breakthrough in drainage, and the size distribution of the residual nonwetting clusters in imbibition. At the macroscopic level, it is suggested that percolation ideas are consistent with the usual multiphase Darcy equations, and critical behaviors of the relative permeability and capillary pressure curves are obtained. By using these results, predictions are made for the shape of the fluid saturation profiles near the percolation thresholds in the presence of buoyancy or viscous pressure gradients. Finally, it is pointed out that very close to the percolation thresholds, the diverging correlation length requires these macroscopic ideas to be modified. A simple way of doing this is suggested.

I. INTRODUCTION

In this paper we consider the displacement of one fluid by another in a porous medium. This process has important practical application in many areas, most particularly in the oil industry where it is the primary mechanism by which hydrocarbons are produced from underground reservoirs. It is also of great interest from the viewpoint of modern physics, since the evolution of the interface between the two fluids provides a physical example of the phenomenon of pattern formation. One such example is the "viscous fingering" which occurs when a less viscous fluid displaces a more viscous one.¹ A second example, which is the topic of the present paper, concerns the percolation phenomena which occur when the fluids are immiscible.

Percolation effects in immiscible displacement in porous media occur when (1) the flow rate and density difference are small, so that at the pore level the pressure drops due to viscosity and buoyancy are small compared to interfacial pressure differences; (2) the medium is random; and (3) the pore space is multiply connected. These percolation effects have been considered by many authors in the past few years.²⁻¹¹ The purpose here is to focus particularly on the observable effects due to the fact that percolation is a critical phenomenon with diverging correlation length and universal critical behavior near the percolation threshold.¹²

We first describe briefly how the above three features lead to a percolation picture of the immiscible displacement process. We consider a porous medium which is filled completely (or perhaps at high saturation) with one fluid of density ρ_1 and viscosity μ_1 which is then flooded with a second fluid of density ρ_2 and viscosity μ_2 at some Darcy velocity (volume flow rate per unit area) V . Crucial to the nature of the displacement process are the wetting characteristics of the fluids and the magnitude of the interfacial tension γ . The fluid in which the contact angle between the fluid-fluid interface and the solid is less than 90° is termed the wetting fluid and the other the nonwet-

ting fluid. If the contact angle is zero we have perfect wetting. When the displacing fluid is the nonwetting fluid the process is called drainage, and when the displacing fluid is the wetting fluid the process is called imbibition.

We consider the case where the viscosities of the fluids are comparable, but $\mu_2 > \mu_1$, so that the displacement is stable and viscous fingering does not occur. The nature of the displacement then depends primarily on the competition between interfacial, buoyancy, and viscous forces. A typical interfacial pressure difference between the phases is of order

$$\Delta p_{\text{int}} \sim \frac{\gamma}{r}, \quad (1.1)$$

where γ is the interfacial tension and r is a microscopic length, for example, a typical grain size in the case of a granular material. Let us define the capillary pressure to be the pressure difference between the nonwetting and wetting phases:

$$p_{\text{cap}} = p_{\text{nw}} - p_w. \quad (1.2)$$

Then in the case of buoyancy, the change in the capillary pressure over a distance r is given by

$$\Delta p_{\text{grav}} = \Delta \rho g r, \quad (1.3)$$

where $\Delta \rho$ is the density difference and g is the acceleration due to gravity. Taking the ratio of (1.1) and (1.3) gives

$$\frac{\Delta p_{\text{grav}}}{\Delta p_{\text{int}}} = \frac{\Delta \rho g r^2}{\gamma} \equiv B. \quad (1.4)$$

The quantity B is called the Bond number, and represents the local competition between buoyancy and interfacial forces.

For the case of viscous pressure gradients, in the applications we consider here it is the pressure drop in the displacing fluid which is important, so the viscous pressure drop across a grain size r may be estimated as

$$\Delta p_{\text{visc}} = \frac{\mu_2 V r}{k}, \quad (1.5)$$

where V is the superficial Darcy velocity of the flood, and k is the permeability of the medium. Taking the ratio of (1.1) and (1.5) gives

$$\frac{\Delta p_{\text{visc}}}{\Delta p_{\text{int}}} = \frac{C}{K}, \quad (1.6)$$

where

$$C = \frac{\mu_2 V}{\gamma} \quad (1.7)$$

is the capillary number expressed in terms of the displacing fluid viscosity and the superficial velocity, and

$$K = \frac{k}{r^2} \quad (1.8)$$

is a geometrical constant. Since the permeability is controlled by the narrow constrictions in the medium, the constant K is typically rather small, of order 10^{-3} .

When the quantities (1.4) and (1.6) are small, the system is in local capillary equilibrium. That is, at a given capillary pressure, the individual menisci separating the two fluids adopt configurations which are determined only by the local geometry, and are independent of the global pressure gradients. Percolation effects arise due to instabilities in the capillary equilibrium: there are certain parts of the pore space which fill with the nonwetting fluid (in drainage) or wetting fluid (in imbibition) not gradually, but suddenly, when the capillary pressure rises above, or drops below, some critical value. Such sudden events are generically called Haines jumps.¹³ A detailed discussion of such mechanisms is given by Lenormand and Zarccone,¹⁰ who point out that some combinations of them are percolationlike, and others are not. Here we will assume the former situation and simply assert that, in both drainage and imbibition, there is a one-to-one correspondence between the capillary pressure p_{cap} and the fraction p of pores (or throats) which are available to the nonwetting fluid (of course the correspondence is different in drainage from in imbibition because the mechanisms are different). In the definition of p we say "available" to mean by virtue of the capillary pressure criterion alone; the actual fraction of pores (or throats) occupied by the nonwetting fluid will be different due to accessibility (i.e., percolation) effects. For simplicity we will often refer to p as the nonwetting fraction.

In the absence of buoyancy or viscous pressure gradients a simple model based on these ideas is the following.^{6,8,9}

(1) Represent the medium as some kind of lattice structure in which the sites represent pores and the bonds throats. Initially the whole lattice is occupied by the displaced fluid, except for one face which is occupied by the displacing fluid. The opposite face is identified as the outlet face from which the displaced fluid escapes.

(2) Assign a random number λ (uniformly in the unit interval) to each site to represent the pressure at which that site will fill with the displacing fluid. (More generally we might assign the random number to the bonds, or to

some combination of the sites and bonds.) More precisely, the number λ for a given site is the fraction of sites which are available to the nonwetting fluid at the capillary pressure at which the site in question fills.

(3) At each time step the displacing fluid configuration grows by occupying the accessible site with the smallest (in drainage) or largest (in imbibition) random number.

(4) Regions of the displaced fluid which become disconnected from the outlet face are "trapped" and cannot be invaded.

(5) The process ends when none of the displaced fluid is connected to the outlet face. The fraction of displaced phase remaining is called the residual saturation.

The above is a modified form of percolation which we call "invasion percolation with trapping." The term "trapping" refers to rule (4), which is concerned with the connectedness properties of the displaced phase. The effect of this rule alone has been considered in Ref. 14. The term "invasion percolation" refers to rule (3) which states that the displacing fluid grows in a single connected cluster along a path of least resistance. Invasion percolation is a kinetic growth phenomenon (as opposed to an equilibrium system such as ordinary percolation) which is of considerable interest in its own right.^{8,15} However, for our purposes the key feature of rule (3) is that the displacing fluid grows in only a single cluster. In fact, a restatement of rule (3) which brings out more clearly the roles of the capillary pressure and available nonwetting fraction is the following.

(3') Gradually increase (in drainage) or decrease (in imbibition) the available nonwetting fraction p (i.e., increase or decrease the capillary pressure) until a site accessible to the displacing fluid becomes available. If this "uncovers" more available sites at the prevailing value of p , then in drainage the sites with the smallest λ value are filled first, and in imbibition those with the largest λ value are filled first. When no more such sites are accessible, the nonwetting available fraction is increased (decreased) again, and so on.

The above model treats drainage and imbibition in essentially the same way. In particular, in both cases there are two percolation thresholds. The first occurs when the displacing fluid first percolates (forms a connected path), and the second when the displaced fluid stops percolating (becomes disconnected). These features are only physically correct if the connectedness of both phases is controlled by the Haines jumps which are the basic ingredient of the percolation model. The point of view taken here is that this is correct for the nonwetting fluid, but not necessarily for the wetting fluid since the latter (at least for small contact angles) can maintain its connectivity through roughness of the pore walls and/or surface films. Thus we will only consider the percolation thresholds corresponding to the nonwetting phase—i.e., the first threshold in drainage and the second threshold in imbibition.

Although invasion percolation with trapping has many of the same qualitative features as ordinary percolation, it cannot be analyzed exactly in terms of usual percolation concepts. This is essentially because the connectedness of the displaced phase is that which occurs in the presence of

only a single cluster of the displacing phase, rather than a randomly placed displacing phase consisting of many clusters as in ordinary percolation. However, at least in the three-dimensional case we are considering here, if we are concerned only with the critical behavior the analysis may be simplified. In drainage we are concerned with the first threshold when the displacing nonwetting phase first percolates. At this stage the nonwetting phase is a fractal and occupies only a vanishingly small fraction of pores. Thus trapping of the wetting phase will be a very rare event and we may safely ignore it—i.e., we may treat the process as invasion percolation without trapping of the other phase. In imbibition we are concerned with the second threshold where the displaced nonwetting phase becomes disconnected. At this stage the wetting fluid will be well above its percolation threshold and so even in ordinary percolation almost all of the wetting phase would be in a single “infinite” cluster—the finite clusters being very small. Thus it is reasonable to expect that, as far as the critical behavior is concerned, the trapping of the displaced nonwetting phase is very similar to that which would occur in ordinary percolation, i.e., we may treat the system as ordinary percolation with trapping of the displaced phase.

In both the drainage and imbibition cases, it is seen that for the purpose of describing the critical behavior near the nonwetting percolation threshold, we may treat the system as if the wetting phase is always perfectly connected, independent of the bulk occupation of the pores. As observed above, this may actually be physically correct when the contact angle is small.

The remainder of this paper is organized as follows. In Sec. II we derive the fundamental macroscopic relation between the fluid saturations and the capillary pressure. In Sec. III we describe certain microscopic (pore level) consequences of percolation effects. In Sec. IV these results are used to derive the shape of the saturation profiles in the presence of buoyancy pressure gradients. In Sec. V we discuss the effect of viscous pressure gradients, and derive the critical behavior of the relative permeability functions. In Sec. VI these results are used to obtain the saturation profiles in the presence of viscous pressure gradients. Some of the results of Secs. IV and VI depend on the way in which the pressure gradients modify the local behavior of the system; in Sec. VII we suggest an approximate way in which these effects may be modeled at the macroscopic level. Finally, Sec. VIII contains a discussion of these results. A glossary of percolation exponents and their values in three dimensions is given in the Appendix.

II. CAPILLARY PRESSURE

As we have seen, the fundamental quantity in the interfacial-tension-dominated regime is the capillary pressure, since it is this quantity to which the system responds. In this section we show the critical behavior of the fluid saturations as a function of capillary pressure. The saturation of each fluid (a macroscopic quantity averaged over many pores) is defined as the fraction of the pore space occupied by that fluid. In a two-phase situa-

tion such as that considered here, the wetting and nonwetting saturations add to unity:

$$S_{nw} + S_w = 1. \quad (2.1)$$

In this paper we will estimate the fluid saturations by counting the fraction of pores occupied by each fluid—i.e., we neglect the size variation of the pores. This should not affect the critical behavior, which is independent of such details.

When discussing the capillary pressure, it is convenient to introduce a dimensionless capillary pressure \hat{p}_{cap} defined by

$$p_{cap} = \frac{\gamma}{r} \hat{p}_{cap}, \quad (2.2)$$

where γ is the interfacial tension, and r is a typical grain size. The dimensionless capillary pressure is then a dimensionless, order-unity function of the nonwetting fraction p .

As in the other sections of this paper, we treat the drainage and imbibition cases separately.

A. Drainage

In drainage we are concerned with the first threshold where the nonwetting fluid first percolates. As discussed in the Introduction, near this threshold we may treat the system as ordinary percolation, but with the displacing fluid occupying only a single cluster. The percolation threshold occurs at some nonwetting available fraction p^* , and a corresponding dimensionless capillary pressure \hat{p}_{cap}^* . If we define

$$\Delta p = p - p^* \quad (2.3)$$

and

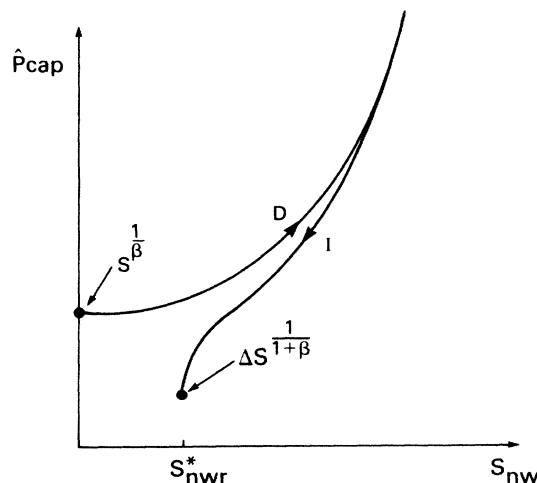


FIG. 1. Dimensionless capillary pressure \hat{p}_{cap} as a function of nonwetting-phase saturation S_{nw} . The curve marked *D* is the drainage curve and that marked *I* is the imbibition curve. The saturation marked S_{nw}^* is the residual nonwetting saturation. The critical behavior is indicated in the figure.

$$\Delta \hat{p}_{\text{cap}} = \hat{p}_{\text{cap}} - \hat{p}_{\text{cap}}^* , \quad (2.4)$$

then we have

$$\Delta \hat{p}_{\text{cap}} \sim \Delta p . \quad (2.5)$$

For an infinite system the nonwetting saturation at the percolation threshold is zero, but as the capillary pressure (and hence the nonwetting fraction) increases, the nonwetting saturation increases as

$$S_{\text{nw}} \sim (\Delta p)^\beta \sim (\Delta \hat{p}_{\text{cap}})^\beta , \quad (2.6)$$

since the nonwetting fluid occupies only the infinite connected cluster. Thus we have

$$\Delta \hat{p}_{\text{cap}} \sim (S_{\text{nw}})^{1/\beta} . \quad (2.7)$$

This behavior is sketched in Fig. 1.

B. Imbibition

In imbibition we are concerned with the second threshold where the nonwetting phase becomes disconnected. Since we will always discuss the drainage and imbibition cases separately, no confusion need arise if we use a similar notation in the two cases. Thus we will again denote the nonwetting fraction at the percolation threshold by p^* , and the corresponding dimensionless capillary pressure by \hat{p}_{cap}^* . Of course, these quantities have different meanings from the drainage case, because the mapping of the system onto the percolation problem is different in the two cases. Again we define

$$\Delta p = p - p^* \quad (2.8)$$

and

$$\Delta \hat{p}_{\text{cap}} = \hat{p}_{\text{cap}} - \hat{p}_{\text{cap}}^* . \quad (2.9)$$

As discussed in the Introduction, near the percolation threshold we may treat the system as ordinary percolation, provided we take into account the trapping of the displaced phase. In percolation with trapping, when we decrease the allowed nonwetting fraction from p to $p - dp$, the wetting-phase saturation increases by an amount $P(p)dp$, since the wetting fluid can only enter the infinite cluster (i.e., the connected portion) of the nonwetting phase.^{7,9,14} Thus, as we approach the percolation threshold,

$$\Delta S_{\text{nw}} \equiv S_{\text{nw}}(p) - S_{\text{nw}}(p^*) = \int_{p^*}^p P(p) dp \sim (\Delta p)^{1+\beta} , \quad (2.10)$$

where $S_{\text{nw}}(p^*)$ is the residual nonwetting saturation S_{nw}^* . Thus the behavior of the capillary pressure near threshold is

$$\Delta \hat{p}_{\text{cap}} \sim \Delta p \sim (\Delta S_{\text{nw}})^{1/(1+\beta)} . \quad (2.11)$$

Since the exponent in (2.11) is less than unity, the capillary pressure has infinite slope at the threshold. This behavior is illustrated in Fig. 1.

III. MICROSCOPIC PREDICTIONS

This section is concerned with the microscopic critical behavior when the effects of pressure gradients due to

buoyancy and viscosity are completely absent. Again, we consider the drainage and imbibition cases separately.

A. Drainage

In drainage we are concerned with the first threshold when the displacing nonwetting fluid first forms a connected path. Since the trapping (if any) of the wetting fluid is not important, the nonwetting fluid is an ordinary percolation cluster at threshold, and so is a fractal. That is, if we choose an origin in the nonwetting fluid, then the volume $M(R)$ of nonwetting fluid within a sphere of radius R grows as^{6,8}

$$M(R) \sim R^D , \quad (3.1)$$

$$r \ll R < L , \quad (3.2)$$

where r is the grain size, L is the sample size, and $D \sim 2.5$ is the fractal dimension of ordinary percolation. As a consequence of this fractal behavior, the nonwetting fluid saturation shows a finite size-scaling effect^{6,8}

$$S_{\text{nw}} \sim L^{D-3} = L^{-\beta/\nu} . \quad (3.3)$$

B. Imbibition

Here we are concerned with the second threshold where the displaced nonwetting phase becomes disconnected. If we let $n(s)$ denote the number of nonwetting clusters containing s pores, then $n(s)$ has the power-law behavior

$$n(s) \sim s^{-\tau} , \quad (3.4)$$

$$1 \ll s \ll s_{\text{max}} , \quad (3.5)$$

where¹⁴

$$s_{\text{max}} \sim L^D , \quad (3.6)$$

and τ is a critical exponent. Previously it was thought,^{8,9} based on computer simulations of invasion percolation with trapping, that τ was around 2.07, less than the corresponding exponent

$$\tau = \frac{3+D}{D} \sim 2.20 \quad (3.7)$$

of ordinary percolation. However, more recent analysis of percolation with trapping¹⁴ suggests that the value should be the same as in ordinary percolation, i.e., 2.20, despite the fact that the actual size distribution is altered by the trapping rule. If we estimate the residual nonwetting saturation S_{nw}^* by counting the number of occupied pores (i.e., we neglect the size variation of the pores) then we have

$$S_{\text{nw}}^* = \sum_{s'=1}^{\infty} s' n(s') . \quad (3.8)$$

Since τ is close to 2, the residual saturation receives contributions from clusters over a wide size range. The best way to estimate the exponent τ , both in experiments and computer simulations, is to compute that part of the residual saturation which is contained in clusters of size greater than s ,

$$m(s) = \sum_{s'=s}^{\infty} s' n(s') \sim s^{2-\tau}, \quad (3.9)$$

$$1 \ll s \ll s_{\max}. \quad (3.10)$$

The finite size of the sample causes the residual saturation to differ from that on an infinite sample by an amount^{9,14}

$$S_{\text{nw}}^* - S_{\text{swr}}(L) \sim L^{-(1+\beta)/\nu}. \quad (3.11)$$

Note that this means that the residual saturation converges much more quickly to its asymptotic value than it would if the size distribution were simply cut off at $s = s_{\max}$, since the latter hypothesis would lead to a behavior $L^{-\beta/\nu}$ for the quantity in (3.11). The result (3.11) is due to the fact that the larger clusters are not entirely missing from the distribution, but are partially broken up into smaller ones.

IV. BUOYANCY EFFECTS

In this section we consider the saturation profiles due to buoyancy pressure gradients. The fundamental assumption is that locally the system responds to the prevailing capillary pressure in the same way as in the absence of the pressure gradient (i.e., as in Sec. II), but that the capillary pressure varies as a function of height:

$$p_{\text{cap}}(z) = p_{\text{cap}}(0) + \Delta\rho g z, \quad (4.1)$$

where z is the vertical height, g is the acceleration due to gravity, and $\Delta\rho$ is the density difference

$$\Delta\rho = \rho_w - \rho_{\text{nw}}. \quad (4.2)$$

Since the capillary pressure is simply related to the saturations via (2.7) or (2.11), it is an easy matter to compute the saturation profiles.

A. Drainage

We assume that the wetting fluid is the heavier fluid and perform the displacement in the vertical direction with the nonwetting fluid introduced from above, so that the displacement is hindered by the buoyancy forces (if the nonwetting fluid were the heavier, we would introduce it from below). Let z denote vertical height and z_0 the lowest height reached by the nonwetting fluid (i.e., the height at which the system is exactly at the percolation threshold). Define

$$\Delta z = z - z_0. \quad (4.3)$$

Thus we have

$$\Delta p_{\text{cap}} \equiv p_{\text{cap}}(z) - p_{\text{cap}}(z_0) = \Delta\rho g \Delta z. \quad (4.4)$$

Expressed in terms of the dimensionless capillary pressure \hat{p}_{cap} this becomes

$$\Delta \hat{p}_{\text{cap}} = B \frac{\Delta z}{r}, \quad (4.5)$$

where B is the Bond number (1.4). From (2.7) we thus have the saturation profile

$$S_{\text{nw}} \sim \left[B \frac{\Delta z}{r} \right]^{\beta}. \quad (4.6)$$

The behavior (4.6) does not hold for all z , but only in some range

$$z_{\min} < \Delta z < z_{\max}. \quad (4.7)$$

If we consider the critical region to extend over the range $\Delta p < \epsilon$, i.e., $S_{\text{nw}} < \epsilon^{\beta}$, then the upper limit is given by

$$\frac{z_{\max}}{r} = \frac{\epsilon}{B}. \quad (4.8)$$

The existence of the lower limit is due to the fact that the pressure gradient modifies the critical behavior close to the threshold. The essential point is that as we approach the percolation threshold the correlation length diverges so that eventually, no matter how small the Bond number, the change in capillary pressure across a correlation length becomes noticeable. Let us denote the local correlation length by ξ . Then, as discussed for the imbibition case in Ref. 9, the system begins to "see" the pressure gradient when Δp becomes so small that the change in p across a correlation length becomes comparable to Δp :

$$\xi \frac{\partial p}{\partial z} \sim \Delta p. \quad (4.9)$$

But from (4.5) we have

$$\frac{\partial p}{\partial z} \sim \frac{\partial \hat{p}_{\text{cap}}}{\partial z} = \frac{B}{r}, \quad (4.10)$$

so that (4.9) becomes

$$\frac{\xi}{r} B \sim \Delta p. \quad (4.11)$$

Since the correlation length scales as

$$\frac{\xi}{r} \sim (\Delta p)^{-\nu}, \quad (4.12)$$

we see that the condition (4.9) is satisfied when

$$\Delta p \sim \Delta p_B \equiv B^{1/(1+\nu)}, \quad (4.13)$$

$$\frac{\xi}{r} \sim \frac{\xi_B}{r} \equiv \left[\frac{1}{B} \right]^{\nu/(1+\nu)}. \quad (4.14)$$

The interpretation of the length ξ_B in (4.14) is that when the correlation length exceeds this value, the system sees the pressure gradient locally. Thus ξ_B is the maximum correlation length which can be developed at a given value of the Bond number B , i.e., it is the maximum length over which the fractal behavior (3.1) can be seen. A useful way to think of this length is as an effective sample size. Since the exponent in (4.14) is around 0.47, this length can be quite small, even for apparently small Bond numbers B . Returning to the saturation profile, we see from (4.5) that when $\Delta p = \Delta p_B$ we have

$$\frac{\Delta z}{r} \sim \frac{\Delta p_B}{B} \sim \left[\frac{1}{B} \right]^{\nu/(1+\nu)} \sim \frac{\xi_B}{r}. \quad (4.15)$$

Thus the lower limit z_{\min} is of the same order as the maximum correlation length

$$\frac{z_{\min}}{r} \sim \frac{\xi_B}{r} = \left[\frac{1}{B} \right]^{\nu/(1+\nu)}. \quad (4.16)$$

Since $\nu/(1+\nu) \sim 0.47$ we see that if $\epsilon \sim 10^{-1}$ and we want the allowed range of z to cover one decade, then we require $B < 10^{-4}$.

B. Imbibition

When the wetting fluid is the heavier fluid we perform the displacement in the vertical direction with the wetting fluid introduced from below. This case was considered in detail in Ref. 9. Here we define z_0 to be the height below which the nonwetting fluid becomes disconnected, and write

$$\Delta z = z - z_0. \quad (4.17)$$

Just as in the drainage case we then have

$$\Delta p_{\text{cap}} = \Delta \rho g \Delta z, \quad (4.18)$$

$$\Delta \hat{p}_{\text{cap}} = B \frac{\Delta z}{r}. \quad (4.19)$$

From (2.11) it follows that the saturation varies with the height as

$$S_{\text{nw}}(z) - S_{\text{nrw}} \sim \left[B \frac{\Delta z}{r} \right]^{1+\beta}. \quad (4.20)$$

As in the drainage case this behavior holds only over some range of z values

$$z_{\text{min}} < \Delta z < z_{\text{max}}. \quad (4.21)$$

By arguments similar to the drainage case, we find that if $\Delta p < \epsilon$ denotes the extent of the critical region, then

$$\frac{z_{\text{max}}}{r} \sim \frac{\epsilon}{B}, \quad (4.22)$$

and that z_{min} is of order

$$\frac{z_{\text{min}}}{r} \sim \frac{\xi_B}{r} \equiv \left[\frac{1}{B} \right]^{\nu/(1+\nu)}, \quad (4.23)$$

i.e., the limits are essentially the same as in the drainage case. The interpretation of the length ξ_B in the imbibition case is that it is the linear dimension of the largest trapped clusters of nonwetting fluid. The nonwetting saturation at $z = z_{\text{min}}$ differs from the residual saturation by an amount

$$\Delta S_{\text{nw}} \sim B^{(1+\beta)/(1+\nu)}. \quad (4.24)$$

As discussed in Ref. 9, another effect of the pressure gradient is to lower the residual nonwetting saturation by an amount of the same order, i.e.,

$$S_{\text{nrw}}^* - S_{\text{nrw}}(B) \sim B^{(1+\beta)/(1+\nu)}. \quad (4.25)$$

V. RELATIVE PERMEABILITIES

In order to compute the effects of viscous pressure gradients in a way analogous to the discussion of buoyancy gradients discussed above, it is necessary to introduce a theoretical picture of how these pressure gradients behave. This is fundamentally more complex than the buoyancy

case because the pressure gradients are dynamically determined by the fluid configurations themselves, rather than being purely hydrostatic as in the buoyancy case. However we will assume that locally the system is in capillary equilibrium, i.e.,

$$p_{\text{nw}} - p_w = p_{\text{cap}}(S), \quad (5.1)$$

where p_{cap} is the same function of saturation as in the absence of pressure gradients. The second assumption is that the flow rates and pressure gradients satisfy the multiphase Darcy equations¹⁶

$$v_i = - \frac{k k_{ri}(S)}{\mu_i} \nabla p_i, \quad (5.2)$$

where v_i is the Darcy velocity of phase i (flow rate per unit area), k is the absolute permeability, k_{ri} is the relative permeability of phase i , and p_i is the pressure measured in the continuous part of phase i . The physical idea behind the relative permeability concept embodied in these equations is that when two fluids are occupying the pore space, the permeability to each is reduced because some of the flow channels are occupied by the other fluid. Since our hypothesis of local capillary equilibrium implies that the fluid configurations are in one-to-one correspondence with the capillary pressure, it follows that at a given local saturation the fluid configurations are always the same (independent of the flow rate), and so the relative permeabilities for a given system are unique functions of saturation. The purpose of this section is to derive the critical behavior of the relative permeability of the nonwetting phase near the percolation thresholds.

A. Drainage

Here we are concerned with the first threshold when the nonwetting fluid first percolates. Close to this threshold the relative permeability to the nonwetting fluid has the behavior

$$k_{\text{mw}} \sim \Delta p^t, \quad (5.3)$$

where t is the conductivity exponent. Combining with (2.6) we then have

$$k_{\text{mw}} \sim (S_{\text{nw}})^{t/B}. \quad (5.4)$$

This behavior is sketched in Fig. 2.

B. Imbibition

Here we are concerned with the second threshold where the nonwetting fluid becomes disconnected. As we approach this threshold, the connected infinite nonwetting cluster is the same as it would have been in ordinary percolation (only the disconnected finite clusters are different). Thus the nonwetting-fluid relative permeability has the behavior

$$k_{\text{nrw}} \sim \Delta p^t, \quad (5.5)$$

where t is the conduction exponent of ordinary percolation. Combining this with (2.10) we have

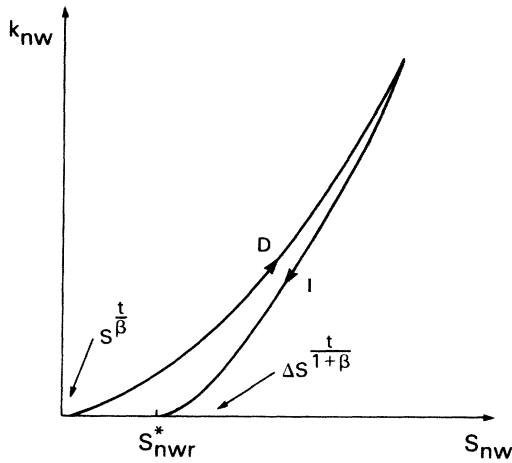


FIG. 2. Nonwetting-phase relative permeability k_{nw} as a function of nonwetting-phase saturation S_{nw} . The curve marked D is the drainage curve and that marked I is the imbibition curve. The saturation marked S_{nwr}^* is the residual nonwetting saturation. The critical behavior is indicated in the figure.

$$k_{nw} \sim (\Delta S_{nw})^{t/(1+\beta)}. \quad (5.6)$$

This behavior is illustrated in Fig. 2.

VI. VISCOUS EFFECTS

In order to compute the saturation profiles in the presence of viscous pressure gradients we have to solve the one-dimensional version of Eqs. (5.1) and (5.2):

$$p_{nw} - p_w = p_{cap}(S), \quad (6.1)$$

$$v_i = -\lambda_i(S) \frac{\partial p_i}{\partial x}, \quad (6.2)$$

where the mobilities λ_i are given by

$$\lambda_i(S) = \frac{kk_{ri}(S)}{\mu_i}. \quad (6.3)$$

These equations are to be solved in conjunction with the continuity equation for each phase:

$$\phi \frac{\partial S_i}{\partial T} + \frac{\partial v_i}{\partial x} = 0, \quad (6.4)$$

where ϕ is the porosity (void fraction) and T is the time. The boundary condition at $x=0$ is

$$v_1 = 0, \quad (6.5a)$$

$$v_2 = V, \quad (6.5b)$$

where V is the total imposed flow rate, and the subscript 1 denotes the displaced fluid and the subscript 2 the displacing fluid. The initial condition on the displacing fluid saturation S_2 is

$$S_2 = S_0, \quad (6.6)$$

where S_0 is some initial constant saturation (possibly zero). In the one-dimensional case we are considering we have from (6.4) and (6.5)

$$v_1 + v_2 = V, \quad (6.7)$$

so that the pressure fields may be eliminated to obtain a single equation for the displacing phase saturation $S \equiv S_2$,

$$\phi \frac{\partial S}{\partial T} + \frac{\partial v}{\partial x} = 0, \quad (6.8)$$

with

$$v \equiv v_2 = VF(S) - G(S) \frac{\partial S}{\partial x}, \quad (6.9)$$

where

$$F(S) = \frac{\lambda_2(S)}{\lambda_1(S) + \lambda_2(S)}, \quad (6.10)$$

$$G(S) = \frac{\lambda_1(S)\lambda_2(S)}{\lambda_1(S) + \lambda_2(S)} \frac{\partial p_{cap}}{\partial S_{nw}}. \quad (6.11)$$

Note that (6.11) is the correct form for both drainage and imbibition, and that the function $G(S)$ is therefore positive in both cases. Equation (6.8) is a nonlinear second-order parabolic differential equation (nonlinear diffusion equation), and except for certain special choices of the relative permeability and capillary-pressure functions cannot be solved exactly.¹⁷ However, at long times it is believed that the saturation profile has the following character.¹⁸ First one draws a tangent to the fractional flow curve $F(S)$ as illustrated in Fig. 3. The point at which the tangent is drawn is called the Buckley-Leverett saturation

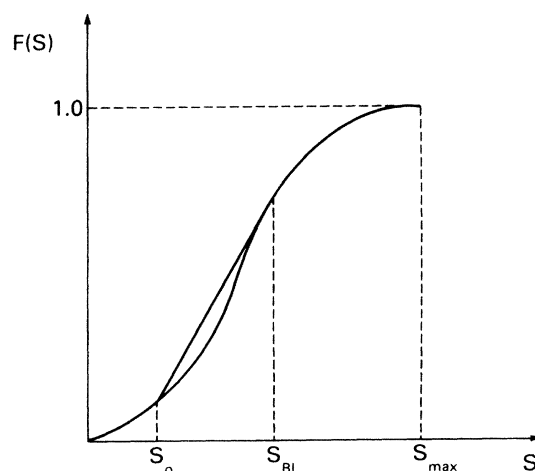


FIG. 3. Fractional flow F [Eq. (6.10)] of the displaced phase as a function of displaced phase saturation S . The Buckley-Leverett saturation S_{BL} is obtained by drawing the tangent to the curve, starting from the point on the curve corresponding to the initial saturation S_0 . If no such tangent can be drawn, S_{BL} is taken to be the initial saturation S_0 . If the chord joining the initial saturation to the maximum saturation S_{max} does not intersect the curve, then S_{BL} is taken to be S_{max} .

S_{BL} . Then the saturations between the initial saturation S_0 and the Buckley-Leverett saturation S_{BL} travel with a common front velocity v_F given by

$$v_F = \frac{V}{\phi} \frac{F(S_{BL}) - F(S_0)}{S_{BL} - S_0}. \quad (6.12)$$

These saturations thus form a traveling wave which advances without change of form. The positions of two saturations S_1 and S_2 differ by an amount

$$x(S_1) - x(S_2) = \int_{S_1}^{S_2} \frac{G(S)}{\phi v_F (S - S_0) - V[F(S) - F(S_0)]} dS, \quad (6.13)$$

where S_0 is the saturation ahead of the traveling front—i.e., the initial saturation. The saturations between S_{BL} and the maximum saturation S_{max} travel with a saturation-dependent velocity given by

$$v(S) = \frac{V}{\phi} \frac{dF}{dS}. \quad (6.14)$$

These saturations thus form a profile which stretches in time:

$$x(S) = v(S)T. \quad (6.15)$$

In the following we will use the solutions (6.13) and (6.15) to derive the shape of the saturation profile (at long times) in the presence of viscous pressure gradients.

A. Drainage

In drainage the displacing fluid is the nonwetting fluid and we assume the initial nonwetting saturation is zero. Since the exponent in (5.4) is greater than unity, the fractional flow curve has zero slope at $S=0$ (i.e., at $S_{nw}=0$) and so it is always possible to draw a tangent to the curve as in Fig. 3—i.e., there is always some range of saturations which form a traveling front. If we let x_0 denote the leading edge of the front, then from (6.13) we have

$$x_0 - x(S) = \int_0^S \frac{G(S)}{\phi v_F S - VF(S)} dS. \quad (6.16)$$

As $S \rightarrow 0$ we have

$$F(S) \sim \frac{\mu_w}{\mu_{nw}} k_{rw}(S) \sim \frac{\mu_w}{\mu_{nw}} S^{t/\beta}, \quad (6.17)$$

$$G(S) \sim \frac{k}{\mu_{nw}} k_{rw}(S) \frac{\partial p_{cap}}{\partial S} \sim \frac{k}{\mu_{nw}} \frac{\gamma}{r} S^{(t+1-\beta)/\beta}, \quad (6.18)$$

so that

$$\Delta x \equiv x_0 - x(S) \sim \frac{\gamma}{\mu_{nw} \phi v_F} \frac{k}{r} S^{(t+1-\beta)/\beta}. \quad (6.19)$$

Thus the desired saturation profile is given by

$$S \sim \left(\frac{C_F}{K} \frac{\Delta x}{r} \right)^{\beta(t+1-\beta)}, \quad (6.20)$$

where C_F is the capillary number expressed in terms of the front velocity and the nonwetting fluid viscosity:

$$C_F = \frac{\mu_{nw} \phi v_F}{\gamma}. \quad (6.21)$$

As in the buoyancy case this behavior only holds for the range of x such that Δp is small enough to be in the critical region, but not so small that the diverging correlation length causes the pressure gradient to be seen at the local level. Let us write the allowed range as

$$x_{min} < \Delta x < x_{max}. \quad (6.22)$$

If we consider the critical region to extend over a range $\Delta p < \epsilon$, i.e., $S < \epsilon^\beta$, then from (6.20) we have

$$\frac{x_{max}}{r} \sim \frac{K}{C} \epsilon^{t+1-\beta}. \quad (6.23)$$

As in the buoyancy case, the lower limit is obtained by solving the equation

$$\xi \frac{\partial p}{\partial x} \sim \Delta p. \quad (6.24)$$

From (2.6) and (6.20) we see that this equation is satisfied when the nonwetting saturation is of order

$$S_{DV} \sim \left(\frac{C_F}{K} \right)^{\beta/(t-\beta+1+\nu)}, \quad (6.25)$$

and the correlation length is of order¹⁹

$$\frac{\xi_{DV}}{r} \sim \left(\frac{K}{C_F} \right)^{\nu/(t-\beta+1+\nu)}. \quad (6.26)$$

As in the buoyancy case, this correlation length is the greatest correlation length which can be developed at the given capillary number. Microscopic effects, such as the fractal behavior (3.1), can be seen only up to this length scale. Since the exponent in (6.26) takes a value around 0.25 this length can be quite short, even for apparently small capillary numbers. Substituting (6.25) in (6.20) we find that the corresponding value of Δx is of the same order as ξ_{DV} , so that x_{min} is given by

$$\frac{x_{min}}{r} \sim \left(\frac{K}{C_F} \right)^{\nu/(t-\beta+1+\nu)}. \quad (6.27)$$

B. Imbibition

In the imbibition case the displacing fluid is the wetting fluid, and the maximum wetting-phase saturation S_{max} is given by

$$S_{max} = 1 - S_{nwr}^*, \quad (6.28)$$

where S_{nwr}^* is the residual nonwetting-phase saturation. Since the exponent in (5.6) is greater than unity, no matter what the initial wetting-phase saturation S_0 , there is always some range of saturations close to S_{max} which form the stretching type of solution. From (5.6) and (6.10) we have as $S \rightarrow S_{max}$,

$$F(S) \sim 1 - \frac{\mu_w}{\mu_{nw}} \frac{k_{rw}(S)}{k_{wr}}, \quad (6.29)$$

where k_{wr} (which is of order unity) is the wetting-phase

relative permeability at residual nonwetting saturation. Thus as $S \rightarrow S_{\max}$,

$$v(S) \sim \frac{V}{\phi k_{wr}} \frac{\mu_w}{\mu_{nw}} (\Delta S)^{[t/(1+\beta)]-1}, \quad (6.30)$$

where ΔS is given by

$$\Delta S = S_{\max} - S = S_{nw} - S_{nwr}^*. \quad (6.31)$$

Thus from (6.15) we have the saturation profile²⁰

$$\Delta S \sim \left[\frac{\phi k_{wr} \mu_{nw} x}{V \mu_w T} \right]^{(1+\beta)/(t-\beta-1)}. \quad (6.32)$$

Note that (at least at this macroscopic level) the residual saturation remains at $x=0$, and does not advance into the sample. As in the other cases, the behavior (6.32) holds only for some range of Δx ,

$$x_{\min} < x < x_{\max}. \quad (6.33)$$

If we consider the critical region to be $\Delta p < \epsilon$, i.e., $\Delta S < \epsilon^{1+\beta}$, then from (6.32) we find that x_{\max} is given by

$$\frac{x_{\max}}{VT} \sim \frac{1}{\phi k_{wr}} \frac{\mu_w}{\mu_{nw}} \epsilon^{t-\beta-1}. \quad (6.34)$$

The lower limit is more complex than in the other cases, because the solution (6.15) is not an exact solution to the macroscopic equations, but only an asymptotic solution for large times. In this solution, the saturation gradient (and hence the capillary pressure gradient) becomes arbitrarily small as $T \rightarrow \infty$, and the pressure gradients in the two fluids are almost equal. However, it was argued in Ref. 9 that near the inlet face where the nonwetting flow velocity v_{nw} is zero, the pressure gradient in the wetting phase always dominates that in the nonwetting phase. Thus, close to residual saturation we have

$$\frac{\partial p}{\partial x} \sim -\frac{r}{\gamma} \frac{\partial p_w}{\partial x} \sim \frac{r}{\gamma} \frac{\mu_w V}{k k_{wr}}. \quad (6.35)$$

As in the drainage case, the system begins to see the pressure gradient when (6.24) is satisfied. In the present imbibition case, use of (6.35) gives⁹

$$\Delta p \sim \Delta p_{IV} \equiv \left[\frac{C}{K_w} \right]^{1/(1+\nu)}, \quad (6.36)$$

with a corresponding correlation length of order

$$\frac{\xi}{r} \sim \frac{\xi_{IV}}{r} \equiv \left[\frac{K_w}{C} \right]^{\nu/(1+\nu)}, \quad (6.37)$$

where C is the capillary number expressed in terms of the wetting fluid viscosity and the total flow rate

$$C = \frac{\mu_w V}{\gamma}, \quad (6.38)$$

and K_w is given by

$$K_w = \frac{k k_{wr}}{r^2}. \quad (6.39)$$

The corresponding saturation value is

$$\Delta S_{IV} = \left[\frac{C}{K_w} \right]^{(1+\beta)/(1+\nu)}. \quad (6.40)$$

Substituting in (6.32) we obtain

$$\frac{x_{\min}}{VT} \sim \frac{1}{\phi k_{wr}} \frac{\mu_w}{\mu_{nw}} \left[\frac{C}{K_w} \right]^{(t-\beta-1)/(1+\nu)}. \quad (6.41)$$

The interpretation of the maximum correlation length ξ_{IV} is that it is the linear extent of the largest trapped clusters. As discussed in Ref. 9, the pressure gradient causes the residual nonwetting saturation to be lowered by an amount of order ΔS_{IV} :

$$S_{nwr}^* - S_{nwr}(V) \sim \left[\frac{C}{K_w} \right]^{(1+\beta)/(1+\nu)}. \quad (6.42)$$

VII. MODIFICATION OF MACROSCOPIC EQUATIONS

The fundamental premise on which this paper is based is that when the pressure gradients due to buoyancy and viscosity are small, the system behaves locally in the same way as in the absence of these gradients—i.e., the system is in local capillary equilibrium. However, we have seen in Secs. IV and VI that as we approach the percolation thresholds this assumption must break down due to the diverging correlation length. The smaller the pressure gradients, the closer we can approach the thresholds, but eventually the system will always begin to see the pressure gradient and the behavior is modified. Strictly speaking, the macroscopic picture must break down when this happens, because there is no length scale larger than the correlation length over which macroscopic variables such as the saturations are effectively constant—i.e., it is impossible to define a macroscopic averaging volume. When the pressure gradients are large, the macroscopic picture becomes completely meaningless, but when they are small one might expect that the effects of the diverging correlation length may be modeled approximately by modifying the capillary pressure and relative permeability functions in the region of the percolation thresholds. This is the purpose of the present section.

The modification we propose here is only appropriate for a one-dimensional flood at constant flow rate, so that the total fluid velocity is fixed by (6.7). Also, for simplicity, we will consider only the situation where viscous pressure gradients alone are acting (i.e., no buoyancy forces). Generalizations to more complex situations may be possible, but will not be considered here. We will consider the imbibition case first, since the observable effects of the pressure gradients are more manifest in that case because the residual saturation is altered.

A. Imbibition

As they system approaches residual saturation, the correlation length increases until the effect of the pressure gradient is seen at the local level. As shown in Sec. VI, this occurs when the saturation reaches a value such that

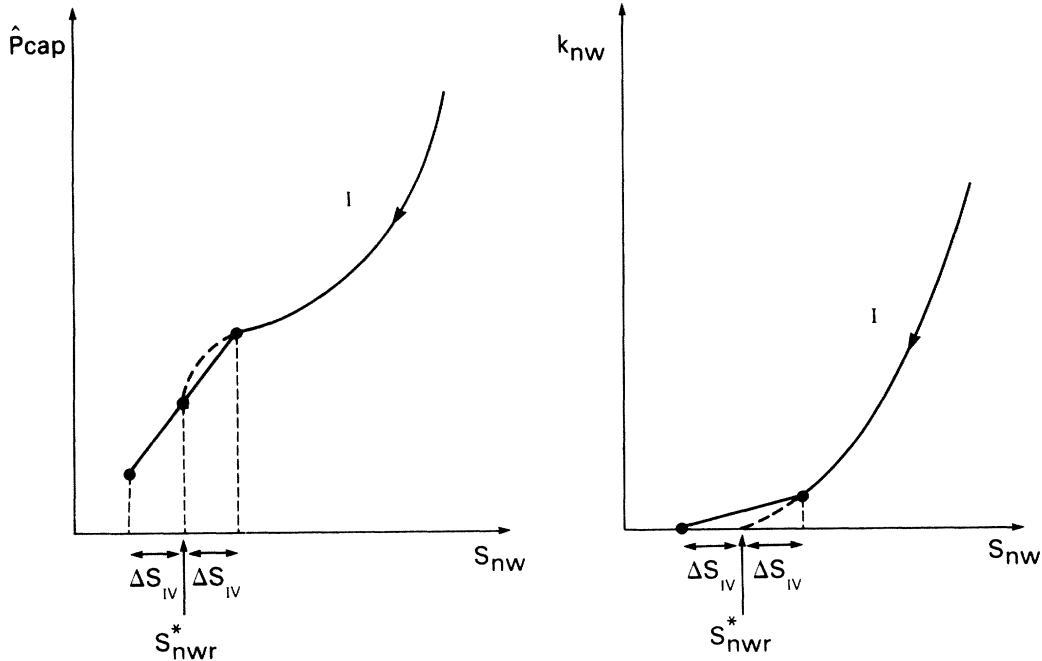


FIG. 4. Modification to the capillary-pressure and nonwetting permeability curves near the residual nonwetting saturation threshold in imbibition. The quantity ΔS_{IV} depends on the flow rate and is defined in (6.40).

$$S_{nw} - S_{nwr}^* = \Delta S_{IV}, \quad (7.1)$$

where ΔS_{IV} is given in (6.40). Once the wetting saturation exceeds this value, the behavior is altered from the zero-gradient situation. In particular, the residual saturation is lowered by an amount of order (6.40). Thus at the very least, the relative permeability and capillary-pressure curves must be modified to accommodate the shifted endpoint. The precise way in which this is done is probably not too important, since the macroscopic equations lose their validity close to the threshold. A simple idea,²¹ illustrated in Fig. 4, is to replace the relative permeability and capillary functions by linear functions in the region $|\Delta S| < S_{IV}$. Note that this modification implies that the velocity $v(S)$ is constant as the system approaches residual saturation. This means that the residual saturation advances into the sample, and regions near the inlet have no continuous nonwetting phase. Of course, this conclusion is due to our simple assumption of a linear relative permeability near the threshold, but it seems physically reasonable.

B. Drainage

The effects of the pressure gradient are not so dramatic in this case because the critical saturation remains at $S_{nw} = 0$. Nevertheless, the behavior must be modified near the threshold. As shown in Sec. VI, the maximum correlation length occurs at a nonwetting saturation

$$S_{nw} = S_{DV}, \quad (7.2)$$

where S_{DV} is given in (6.25). Again, a simple possibility is to replace the relative permeability and capillary-pressure functions by straight lines in the region $S_{nw} < S_{DV}$ as illustrated in Fig. 5. This modification causes the saturation profile near the threshold to be linear, as can easily be checked by repeating the steps (6.17)–(6.20) for the modified relative permeability and capillary-pressure functions.

VIII. DISCUSSION

The purpose of this paper has been to present a variety of theoretical predictions of percolation models of immiscible displacement in porous media. These predictions are of three main types: (a) microscopic predictions such as fractal dimensions and cluster size distributions, (b) critical behavior of the macroscopic capillary-pressure and relative permeability functions, and (c) shapes of the saturation profiles in the presence of pressure gradients due to buoyancy and viscosity. The beauty of these predictions is that they are *universal*—i.e., do not depend on the details of the porous medium and the fluids.

If these percolation effects are not seen, it is possible to identify three possible reasons.

(1) The physics of the models is wrong. This is most likely to occur in the imbibition case, where the displacement mechanisms are more complex. In particular, the displacement may occur via multiple mechanisms, whose combined effect is not percolationlike.¹⁰

(2) The pressure gradients due to buoyancy and viscosity are too strong, so that the critical behavior is smeared.

(3) If percolation effects are to be seen over a correla-

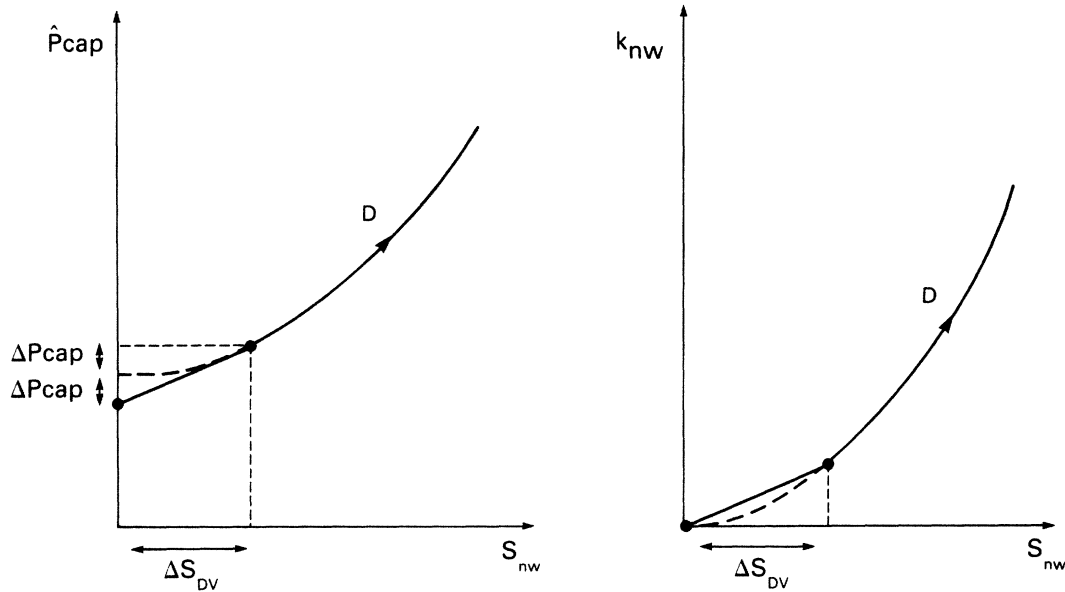


FIG. 5. Modification to the capillary-pressure and nonwetting permeability curves near the nonwetting injection threshold at $S_{nw} =$ in drainage. The quantity ΔS_{ID} depends on the flow rate and is defined in (6.25).

tion length ξ , then the medium must be statistically homogeneous over that scale. This may not be the case.

Despite these difficulties, critical percolation effects have been observed in drainage in two-dimensional artificial porous media. In particular, Lenormand and Zarcone²² have shown the fractal dimension of the displacing nonwetting fluid in drainage to be around 1.82, in good agreement with computer simulations of invasion percolation with trapping in two dimensions.^{6,8} To make the corresponding measurements in three dimensions requires pore-level observation of the system. The size distribution of the residual nonwetting clusters in imbibition has been measured by a destructive technique by Chatsis and Morrow,²³ but the data were not analyzed in terms of percolation ideas. While the predictions for critical behaviors of the capillary-pressure and relative permeability functions are in qualitative agreement with commonly used functions based on experiments, these experiments are not of sufficient precision to pick out the correct critical behavior near the threshold. One reason for this is that the experiments do not usually make saturation measurements inside the sample, but rather rely on external measurements which are strongly affected by boundary effects. For this reason there seems more hope for seeing the critical behavior in the saturation profiles, which are true bulk effects in which the capillary pressure, and hence saturations, are modulated by the physical pressure gradients themselves rather than by external forces. Some initial results for drainage in the presence of buoyancy have been obtained by destructive technique (using Woods metal as the nonwetting phase) by Clement, Baudet, and Hulin.²⁴ A promising nondestructive technique using a transparent porous medium and laser-induced fluorescence has been developed by Chen and Wada.²⁵ All of the

above-mentioned techniques give pore-level resolution and can be used to test the microscopic predictions of percolation. However, if the pressure gradients are small enough, the critical behavior of the saturation profiles may extend over macroscopic distances and be observed by macroscopic imaging techniques such as x-ray and NMR tomography.

APPENDIX

In this appendix we summarize our definitions of the critical exponents of percolation, and their approximate values in three dimensions.²⁶ We denote the occupation fraction by p and the critical fraction by p^* and write

$$\Delta p = p - p^* .$$

In our applications we are always above threshold, so Δp is positive. The order parameter $P(p)$ is the fraction of occupied sites in the infinite cluster and scales as

$$P(p) \sim (\Delta p)^\beta ,$$

where $\beta \sim 0.45$. If the occupied sites are conducting and the empty sites insulating, then the conductivity Σ scales above threshold as

$$\Sigma \sim (\Delta p)^t ,$$

where $t \sim 1.9$ is the conductivity exponent. The correlation length L , which may be taken as the typical size of the finite clusters, diverges as

$$L \sim (\Delta p)^{-\nu} ,$$

where $\nu \sim 0.88$. At threshold the infinite cluster is a fractal with fractal dimension

$$D = 3 - \frac{\beta}{\nu} \sim 2.5 .$$

Finally, at threshold the number of finite clusters of size s scales as

$$n(s) \sim s^{-\tau} ,$$

where

$$\tau = \frac{3+D}{D} = \frac{6\nu-\beta}{3\nu-\beta} \sim 2.20 .$$

-
- ¹L. Paterson, Phys. Rev. Lett. **52**, 1621 (1984); J. Nittman, G. Daccord, and H. E. Stanley, Nature (London) **314**, 141 (1985); J.-D. Chen and D. Wilkinson, Phys. Rev. Lett. **55**, 1892 (1985); K. J. Maloy, J. Feder, and T. Jossang, *ibid.* **55**, 2688 (1985); J. Sherwood and J. Nittmann, J. Phys. (Paris) **47**, 15 (1986).
- ²J. C. Melrose and C. F. Brandner, Can. J. Petrol. Tech. **13**, 54 (1974).
- ³P. G. de Gennes and E. Guyon, J. Méc. **17**, 403 (1978).
- ⁴R. Lenormand and S. Bories, C. R. Acad. Sci. **291**, 279 (1980).
- ⁵R. G. Larson, L. E. Scriven, and H. T. Davis, Chem. Eng. Sci. **36**, 57 (1981); R. G. Larson, H. T. Davis, and L. E. Scriven, *ibid.* **36**, 75 (1981).
- ⁶R. Chandler, J. Koplik, K. Lerman, and J. Willemsen, J. Fluid Mech. **119**, 249 (1982).
- ⁷R. G. Larson and N. Morrow, Powder Tech. **30**, 123 (1981).
- ⁸D. Wilkinson and J. Willemsen, J. Phys. A **16**, 3365 (1983); J. Willemsen, Phys. Rev. Lett. **52**, 2197 (1984).
- ⁹D. Wilkinson, Phys. Rev. A **30**, 520 (1984).
- ¹⁰R. Lenormand and C. Zarccone, Society of Petroleum Engineers paper No. 13264, Houston, Texas, 1984 (unpublished).
- ¹¹T. S. Ramakrishnan and D. T. Wasan, Int. J. Multiphase Flow (to be published).
- ¹²A preliminary version of some of this work has been reported previously: D. Wilkinson, in *Physics of Finely Divided Matter*, edited by N. Boccaro and M. Daoud (Springer-Verlag, New York, (1985).
- ¹³W. B. Haines, J. Agricult. Sci. **20**, 97 (1930).
- ¹⁴M. Dias and D. Wilkinson, J. Phys. A (to be published).
- ¹⁵B. Nickel and D. Wilkinson, Phys. Rev. Lett. **51**, 71 (1983).
- ¹⁶See, for example, A. Scheidegger, *The Physics of Flow Through Porous Media* (University of Toronto, Toronto, 1974).
- ¹⁷Exact solutions to these equations have been found for special cases of the relative permeability and capillary-pressure functions: A. S. Fokas and Y. C. Yortsos, SIAM J. Appl. Math. **42**, 318 (1982); M. King, J. Math. Phys. **26**, 870 (1985).
- ¹⁸S. E. Buckley and M. C. Leverett, Trans. AIME **146**, 107 (1942); H. J. Welge, *ibid.* **192**, 91 (1952). For a discussion, see H. J. Morel-Seytoux, in *Flow Through Porous Media*, edited by R. de Wiest (Academic, New York, 1969).
- ¹⁹The existence of this maximum correlation length has been derived in a somewhat different way by deGennes [P.-G. de Gennes (private communication)].
- ²⁰This result has also been obtained by deGennes [P.-G. de Gennes (private communication)].
- ²¹A more sophisticated idea, based on using scaling functions with $\Delta S/\Delta S_{IV}$ as the scaling variable, is suggested by some ideas of Clement [E. Clement (private communication)].
- ²²R. Lenormand and C. Zarccone, Phys. Rev. Lett. **54**, 2226 (1985).
- ²³I. Chatsis, M. S. Kuntamukkula, and N. R. Morrow, Society of Petroleum Engineers Paper No. 13213, Houston, Texas, 1984 (unpublished).
- ²⁴E. Clement, C. Baudet, and J.-P. Hulin, J. Phys. (Paris) Lett. **46**, L1163 (1985).
- ²⁵J.-D. Chen and N. Wada, Exp. Fluids (to be published).
- ²⁶For a review of percolation theory, see D. Stauffer, Phys. Rep. **54**, 1 (1979).